Acta Scientiarum
http://periodicos.uem.br/ojs
ISSN on-line: 1807-8664
Doi: 10.4025/actascitechnol.v44i1.57818

Carbon nanotubes added to Portland cement pastes containing nano-silica

Thiago Melanda Mendes[1*] and Wellington Longuini Repette[2]

[1]Departamento de Engenharia Ambiental, Universidade Tecnológica Federal do Paraná, Avenida dos Pioneiros, 3131, 86036-370, Londrina, Paraná, Brazil. [2]Departamento de Engenharia Civil, Universidade Federal de Santa Catarina, Florianópolis, Santa Catarina, Brazil. *Author for correspondence. E-mail: thiagomendes@utfpr.edu.br

ABSTRACT. This study assesses the effect of size, as well as binary and ternary mixtures of three different carbon nanotubes added to Portland cement pastes containing nano-silica. Carbon nanotubes were characterized in terms of size and morphology by transmission electron microscopy, particle size distribution by laser granulometry and electroacoustic attenuation spectroscopy and specific surface area by gas adsorption. The combination of more than one characterization technique helps to identify the finer or coarser carbon nanotube suspensions. The use of low amount of carbon nanotubes and nano-silica does not affect the rheological properties of cementitious matrices. The compressive strength decreases, but flexural strength improves for the finer carbon nanotube. The microstructural analysis showed the adherence of carbon nanotubes on the surface of matrix's particles, and the nucleation of hydration products on the surface of carbon nanotubes.

Keywords: particle size; rheological properties; mechanical properties; microstructure.

Received on February 15, 2021.
Accepted on October 25, 2021.

Introduction

The reinforced and pre-stressed concrete are the most widely used composite materials in construction. However, nowadays metallic, mineral or organic fibers have been used to improve the ductility and tenacity of these composite materials. Carbon nanotubes have excellent mechanical performance with a tensile strength ranging from 55.8 to 89.9 GPa; a high modulus of elasticity around 1 TPa (970 GPa); and high deformability varying from 6.8 to 13.7% (Chang et al., 2010). Density of 2100 g cm^{-3} is another important characteristic of this reinforcement material (Nanostructured & Amorphous Materials, 2021). For these reasons carbon nanotubes have been extensively studied to allow the use of these high strength fibers, as a reinforcement for cement-based materials.

In most published research, the characterization of the material was obtained from the supplier's information. The transmission and scanning electron microscopies are commonly performed to verify the particle size and morphology. The particle size distribution can be performed with dynamic lightening scattering (DLS), centrifugal liquid sedimentation or spectroscopy of electroacoustic attenuation. Furthermore, when they are used in conjunction with the specific surface area, measured by gas adsorption, it is a useful tool to provide the characterization of carbon nanotubes. The sample preparation methods influence not only the measurements, reducing its size due to the dispersion process, but they also may lead to the rupture or breakdown of carbon nanotubes as discussed by Sobolkina et al. (2012) and Yakovlev et al. (2017).

The specific surface area of nano inclusions has a direct effect on rheological properties, and the consumption of dispersant is closely related to the content of carbon nanotubes (Meng & Khayat, 2016; El-Gamal, Hashem, & Amin, 2017; Siroka et al., 2019). Mixtures containing a low amount of carbon nanotubes can present rheological behavior like cement paste without nano inclusions. Nevertheless, when the content of carbon nanotubes increases, there is a considerable changing in the workability or fluidity of cement-based materials (Collins, Lambert, & Duan, 2012; Medeiros, Dranka, Mattana, & Costa, 2015; Skripkiunas, Karpova, Barauskas, Bendoraitiene, & Yakovlev, 2018; Leonavicius et al., 2018; Farooq et al., 2020).

The incorporation of carbon nanotubes affects the cement-based materials mechanical performance. The mechanical properties of these nanocomposites present an optimum content, which varies according to the type of carbon nanotubes and water/cement ratio (Yazdanbakhsh & Grasley, 2012). However, the specific surface area of the particles, as well as the size and dispersed or agglomerates conditions of the carbon

nanotubes must be considered. Some studies have shown a considerable gain in flexural strength, varying from 6 to 43% (Navid et al., 2016). Other studies have shown results of compressive or flexural strength lower than the reference mixtures, without carbon nanotubes (Collins et al., 2012; Jung, Oh, Kim, & Moon, 2019), or even different mechanical behaviors of these composites under compression or under flexural stress (Hu, Luo, Li, Li, & Sun, 2014).

The agglomerates of carbon nanotubes were clearly observed in scanning electron micrographies published by Hawreen, Bogas, and Dias (2018), but well dispersed carbon nanotubes, individual particles with few micrometers, were observed by Sobolkina et al. (2012). The interface transition zone (ITZ) between carbon nanotubes and matrix is a key factor for improving the microstructure of these composites. The functionalization of carbon nanotube surface using polymers, employed by Cwirzen, Cwirzen, and Pentalla (2015), as well as the shell of nano-silica studied by Siroka et al. (2019), contribute to the improvement of the adhesion between the matrix and carbon nanotubes. The nucleation is another important effect of carbon nanotube on the microstructure of these composites, as observed by El-Gamal et al. (2017); and Jung et al. (2019), allowing the growth of hydration products such as C-S-H/C-A-H/CH on the surface of carbon nanotubes. The effect of size of carbon nanotubes was evaluated by Konsta-Gdoutos, Metaxa, and Shah (2010a; 2010b) and Al-Rub, Ashour, and Tyson (2012), and the combined effects of carbon nanotubes and nano-silica were evaluated by Yakovlev et al. (2017); Siroka et al. (2019) and Mendoza, Sierra, and Tóbon (2014). Most available references compared different types of carbon nanotubes, varying their size or functionalization types. There are not references about the combined effects of nanosilica with carbon nanotubes with different sizes, as well their combination in binary and ternary mixtures of carbon nanotubes with different sizes and nano-silica. Thus, this study characterized the morphology, particle size and specific surface area of three different carbon nanotubes. In order to evaluate the effect of size, as well as binary and ternary mixture of these three different carbon nanotubes on the rheological and mechanical properties, and also on the microstructure of Portland cement pastes containing nano-silica.

Material and methods

Three different aqueous suspensions of multi-walled carbon nanotubes (MWCNT) were obtained from Nanostructured & Amorphous Materials. They were named CNT_1, CNT_2 and CNT_3, and their characteristics are listed in Table 1. Table 2 presents the other materials employed in this study, and their physical characteristics. The specific surface area was measured by gas adsorption (B.E.T), samples were dried in an oven at 105ºC, and kept under a vacuum of 68.9 Pascal, at 60ºC for 24 hours, using a BELSORP MAX equipment. Densities of Portland cement, basaltic filler and silica fume were determined by the picnometry of liquids according to ABNT NBR 16605 (*Associação Brasileira de Normas Técnicas* [ABNT], 2017). For nano-silicas Cembinder 8 (nS_1), Cembinder 30 (nS_2) and Cembinder 50 (nS_5), the density of solids was calculated from the suspension densities and the mass concentrations: 1.4 g cm^{-3} and 50 *wt.*%, 1.20 g cm^{-3} and 30 *wt.*%, 1.05 g cm^{-3} and 15 *wt.*%, respectively. The density of the carbon nanotubes was obtained from the supplier. Polycarboxilic acid superplasticizer was used as a dispersing additive, with a density of 1.06 g cm^{-3} and solid concentration of 35.42 *wt.*%.

Table 1. Physical characteristics of MWCNT (Nanostructured & Amorphous Materials, 2021).

Description	CNT_1	CNT_2	CNT_3
Diameter (nm)	> 50	20-30	30-50
Length (mm)	10-20	10-30	10-20
Specific surface Area (m^2 g^{-1})	43.00	55.94	39.38
Density (g cm^{-3})	2.10	2.10	2.10
Solids concentration (*wt.*%)	7-8	3	1

Table 2. Physical characteristics of raw materials.

Description	Density (g cm^{-3})	Specific Surface Area (m^2 g^{-1})
Portland cement	3.05	1.25
Silica Fume	2.20	14.4
Basaltic filler	2.85	1.14
Cembinder 8	2.33	47.3
Cembinder 30	2.25	88.9
Cembinder 75	2.53	44.6

The particle size distributions of carbon nanotubes were determined with a laser granulometer Malvern 2200 for samples diluted in deionized water, and spectroscopy of electroacoustic attenuation, as for the samples received from the supplier, they were not diluted. The Transmission Electron Microscopy (TEM) of carbon nanotubes and nano-silicas suspensions was carried out with Fei Tecnai G2 equipment, operating at 80 and 120 kV. The samples of carbon nanotubes and nano-silica were diluted with deionized water at a 1 mg mL^{-1} and sonicated during 30 min. Five milliliters (5µL) of these diluted suspensions were dropped into a copper-carbon grid (300 mesh), and covered with polyvinyl formal resin, commonly called Formvar.

Table 3 presents the reference matrix (M) without carbon nanotubes, and composites formulated with 0.05 *wt*.% of CNT_1 (C_1), CNT_2 (C_2) and CNT_3 (C_3). In addition, the composites formulated with a binary mixture containing 0.05 *wt*.% of CNT_1 and 0.025 *wt*.% of CNT_2 (C_{12}); and with a ternary mixture containing 0.05 *wt*.% of CNT_1, 0.025 *wt*.% of CNT_2 and 0.0125 *wt*.% of CNT_3 (C_{123}). The dispersant content was fixed at 2 *wt*.% of solid mass, and the water/solids ratio 0.30 was kept constant. For all mixtures, the water content of the dispersant, nano-silica and carbon nanotubes suspensions was subtracted from the total amount. Solids were considered as the sum of Portland cement, basaltic filler, silica fume, nano-silicas and carbon nanotubes.

The suspensions of nano-silicas, carbon nanotubes and the dispersant were previously diluted in deionized water. The mixing was performed in a laboratory mixer employing a rod of 6 cm diameter axial flow, cawles model, applying the following process: (i) dry powder was mixed at 586 rpm for 60 s; (ii) 2/3 of the suspension (water + dispersant + nano-silicas + carbon nanotubes) was added and mixed at 586 rpm for 120 s; (iii) 1/3 of the suspension was added (water + dispersant + nano-silicas + carbon nanotubes) and mixed at 586 rpm for 120 s. For each batch, content varying between 625 and 650 g was mixed.

A temperature-controlled rheometer with parallel plates geometry was used to measure the rheological properties of pastes. The plates have a diameter of 25 mm, and a surface texture of serrated crosshatched to avoid 'wall slip'. The applied gap between plates was 1 mm. Flow curves were obtained using a shear rate controlling, varying from 10 and 100 s^{-1}, in 10 s^{-1} intervals. The shear rate (γ) was increased from 10 to 100 s^{-1} (upper curve) and reduced from 100 to 10 s^{-1} (downs curve). Pastes were maintained 30 seconds at each shear rate; values were recorded at last 3 s. The yield stress (τ_0) and the plastic viscosity (η) were calculated using the Bingham Equation ($\tau = \tau_0 + \gamma^* \eta$), considering the downs curve. All rotational rheometry tests were conducted at 23ºC, after 10 min. of water addition into the powder.

Three prismatic samples (2x2x10 cm) and eight cylinders samples (2x5 cm) of cement paste were molded by casting; manually compacted was applied in order to avoid molding defects. Specimens were maintained at 23ºC during 24 hours, and immersed in saturated calcium hydroxide solution at 85ºC during 18 hours. Compressive strength of mixtures was measured in six cylindrical specimens, which had the upper face sliced with water-cooled disk, resulting in a final height of 4 cm. Compressive and flexural strengths were measured using a universal testing machine, applying loading rates of 1.0 (Graybeal, 2014) and 1.25 MPa s^{-1} (American Society for Testing and Materials [ASTM], 2018), respectively.

For the microstructural analysis, inner prismatic specimens (10x10x20 mm) were extracted from two cylindrical samples, which were maintained at the same curing conditions described before. For scanning electron microscopy, the prismatic specimens were broken, and a small inner part was used. Samples were analyzed by scanning electron microscopy (SEM) using Quanta 600 FEI-Philips equipment operating at 30 kV. Gold treatment was employed on the specimens' surface.

Table 3. Compositions by mass (*wt*.%) mixtures.

Description	M	C_1	C_2	C_3	C_{12}	C_{123}
Portland cement	49.95	49.94	49.95	49.95	49.95	49.95
Basaltic filler	24.92	24.91	24.92	24.92	24.92	24.92
Silica fume	24.92	24.91	24.92	24.92	24.92	24.92
Cembinder 8	0.08	0.07	0.08	0.08	0.08	0.08
Cembinder 30	0.10	0.09	0.10	0.10	0.10	0.10
Cembinder 50	0.03	0.02	0.03	0.03	0.03	0.03
CNT_1	0.00	0.05	0.00	0.00	0.05	0.05
CNT_2	0.00	0,00	0.05	0.00	0.025	0.025
CNT_3	0.00	0.00	0.00	0.05	0.00	0.0125

Results and discussion

Figure 1 presents the transmission electron micrographies of carbon nanotubes 1 (CNT_1). As seen in Figure 1a, it is possible to observe a micrometric agglomerate of nanotubes with a few micrometers, more than 11 μm. Figure 1b also showed a micrometric particle of carbon nanotubes in the suspension, close to a larger agglomerate, and surrounded by many individual carbon nanotubes. Figure 1c reveals some tangled carbon nanotubes, with a micrometric length and a diameter of a few nanometers. Two carbon nanotubes are shown in Figure 1d, which have similar diameters, 37 and 30 nm, but lengths are clearly different. Figure 1e and f showed carbon nanotubes, with a length around 300 nm (0,3 μm) and a diameter less than 25 nm.

Figure 2 shows the transmission electron micrographies of carbon nanotubes 2 (CNT_2). The presence of micrometric particles can also be seen in Figure 2a, which is composed of many carbon nanotubes. Figure 2b reveals that carbon nanotubes can have different shapes, such as rolled or stretched fibers, with many diameters and lengths. Figure 2c showed a long fiber with a micrometer length (> 2.1 μm) and a nanometric diameter, less than 26 nm, as seen in Figure 2e. Many other fibers length and diameters of fibers can be seen in Figure 2d, ranging from a few micrometers or even a few nanometers. Figure 2f showed that the diameters of CNT_2 vary between 53 nm and 39 nm.

Figure 3 shows the transmission electron micrographies of carbon nanotubes 3 (CNT_3). Figure 3a also revealed the presence of micrometric agglomerates of carbon nanotubes, surrounded by many clusters of carbon nanotubes. Figure 2b showed that this agglomerate is composed mainly by interlace nanotubes, in this case, this particle is smaller than 1 μm. Figure 3c showed different particles shapes and lengths, ranging from micrometric sizes to nanometric particles. In addition, that these particles diameters can also vary from 39 to 15 nm or less, Figure 3e. Figure 3d also shows carbon nanotubes with different diameters, the coarsest particle with a diameter around 32 nm, while the smaller has a diameter around 15 nm. Figure 3f revealed another small carbon nanotube with a length around 150 nm (0,15 μm) and a diameter about 13 nm, and the presence of an even smaller particle next to it, probably a fragment of carbon nanotube due to the sonication process as observed by Sobolkina et al. (2012) and Yakovlev et al. (2017).

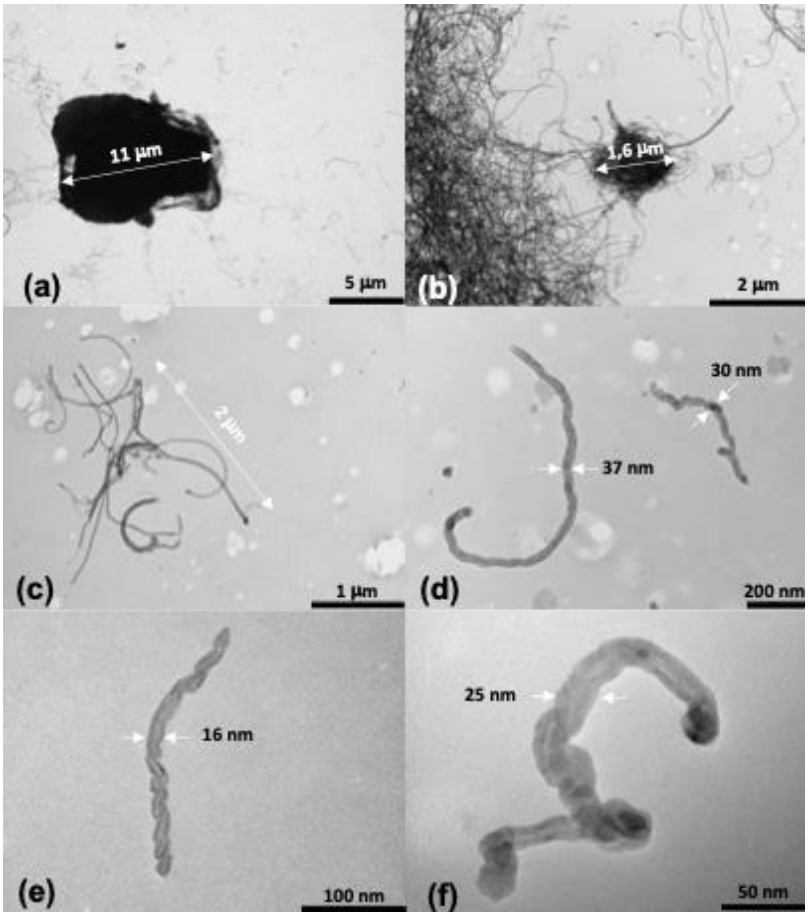

Figure 1. Transmission electron micrographies of CNT_1.

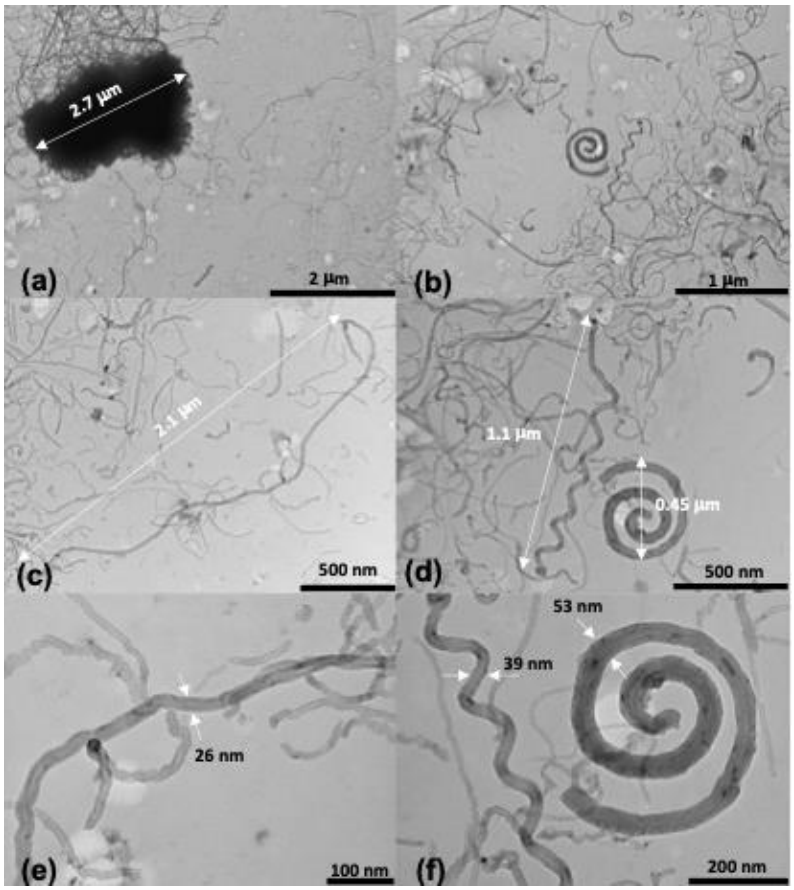

Figure 2. Transmission electron micrographies of CNT_2.

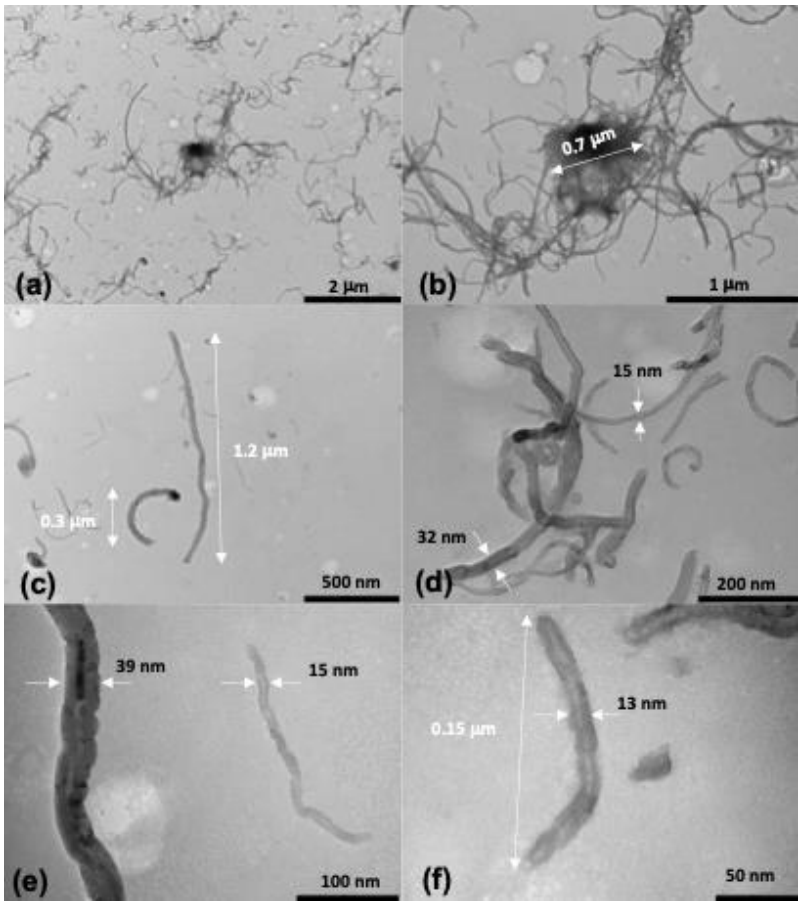

Figure 3. Transmission electron micrographies of CNT_3.

Figure 4 shows the transmission electron micrographies of nano-silicas Cembinder 8 (a, b), Cembinder 30 (c, d) and Cembinder 50 (e, f). As it was seen, the nano-silica Cembinder 8 (nS_1) is the coarse granulometry. Figure 4a and b showed the presence of particles with a diameter around 100 nm or less for nano-silica Cembinder 8. Figure 4b and c revealed that nano-silica Cembinder 30 (nS_2) presented a granulometry finer than nano-silica Cembinder 8, with all particles smaller than 30 nm. While nano-silica Cembinder 50 (nS_3) is clearly composed by an agglomerate of nanoparticles, these agglomerates vary around 70 nm. Thus, comparing the particle size of carbon nanotubes and nano-silicas, they have the same order of magnitude, allowing physical interactions between fibers reinforcement and cementitious matrix.

Figure 5a and b show the particle size distribution of carbon nanotubes, obtained by laser granulometer and electric-acoustic attenuation methods. As seen in Figure 5a, carbon nanotubes have micrometric particles ranging from 1 to 100 μm and another particles population smaller than 1 μm. Carbon nanotubes showed a similar particle size distribution in both methods, CNT_1 is coarser than CNT_2 and CNT_3. These particles size distributions are in accordance with the size of carbon nanotubes observed in the micrographies. The presence of micrometric particles, mainly composed by agglomerates of carbon nanotubes, was observed in Figure 1a and b, Figure 2a and Figure 3a and b. The micrometric particles, may also be composed of the individual or tangled particles of carbon nanotubes, as seen in the Figure 1c and d, Figure 2c and d, and Figure 3c and d. The nanometric particles, mainly those which present a size smaller than 200-300 nm observed in the granulometric distributions, were also observed in the micrographies. As seen in Figure 1d, e and f, Figure 2e and f, and also in Figure 3d, e and f. These results help to understand the condition of these carbon nanotubes in the suspensions. And when two or more characterization techniques were combined, they may help to improve selecting process of the supplier of carbon nanotubes and their products.

Figure 6 shows the flow curves of the studied mixtures. It was observed that the amount of polycarboxylate dispersant caused the non-occurrence of yield stress for the evaluated mixtures. The viscosity of all studied mixtures is lower than the reference cement paste (M). Carbon nanotubes 3 (CNT_3) led to the better fluidity (1/viscosity) for the studied cement pastes, due to the reduction of 63% in the viscosity as a result of the smaller number of micrometric particles, as seen in Figure 5 a and b. Carbon nanotubes 2 and 1 had viscosity values 16 and 33% lower than reference mixture, but CNT_2 had the largest specific surface area, reducing the separation between particles. When combined in the C_{12} mixture, the viscosity of this paste was 26% lower than reference, intermediate value between the viscosity of the C_1 and C_2 mixtures, due to the greater amount of carbon nanotubes (0.075 *wt*.%). For the composition C_{123}, containing 0.0875 *wt*.% of the three carbon nanotubes, the viscosity of cement paste has the same value as the binary mixture C_{12}. This trend of reducing the viscosity of cement pastes containing carbon nanotubes was also observed by Leonavicius et al. (2018), who attribute it to the effects of surfactants commonly used to disperse the carbon nanotubes. Thus, the type and quantity of Dimethylformamide or methyl-2-pyrrolidinone surfactants used by the supplier can explain the differences observed, even for the low amounts of carbon nanotubes and concentrations of surfactant.

Figure 7 shows the mechanical properties of the reference matrix and composites containing carbon nanotubes. The addition of 0.05 *wt*.% of carbon nanotubes CNT_1, CNT_2 and CNT_3 leads to a 14 to 21% reduction in the compressive strength of composites C_1, C_2 and C_3, as seen in Figure 7a. When the binary mixture containing 0.05 *wt*.% of CNT_1 and 0.025 *wt*.% of CNT_2, and the ternary mixture containing 0.05 *wt*.% of CNT_1, 0.025 *wt*.% of CNT_2 and 0.0125 *wt*.% of CNT_3, were incorporated in the composites C_{12} and C_{123}, the compressive strength is 6 and 4% less than the reference matrix, which can be considered similar to the reference mixture without carbon nanotubes. The use of carbon nanotubes, and indirectly the presence of the surfactants additives, even for very low quantities shall result in the higher incorporation of entrapped air for the composites. It was expected that the suspension of carbon nanotubes 3 (CNT_3) needs a higher amount of the surfactant due to its thicker granulometry. Similarly, the suspension of carbon nanotube 2 (CNT_2) may present a quantity of surfactant higher than the suspension of carbon nanotubes 1 (CNT_1), which may explain the reduction of compressive strength according to the granulometry of the carbon nanotubes. The incorporation of carbon nanotubes increased the solid concentration of cement paste due its lower density (2.100 g cm^{-3}), when compared to the other solids which compose it, such as cement, basalt filler, silica fume and nano-silica. As the content of carbon nanotubes rises, the negative impact of the air incorporation of surfactant, may be compensated by the higher solid concentration.

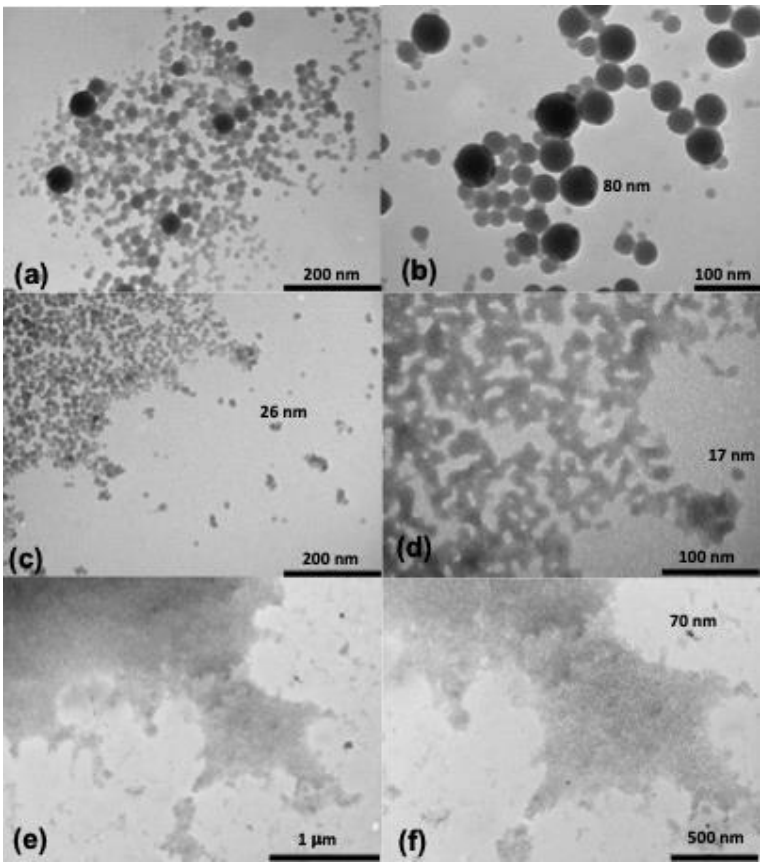

Figure 4. Transmission electron micrographies of nano-silicas (a, b) Cembinder 8, (c, d) Cembinder 30, (e, f) Cembinder 50.

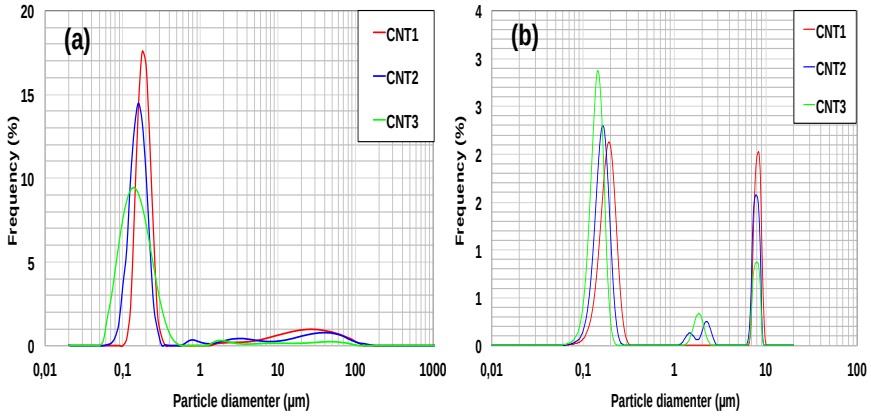

Figure 5. Particle size distribution of carbon nanotubes (a) laser granulometry (b) electric-acoustic attenuation.

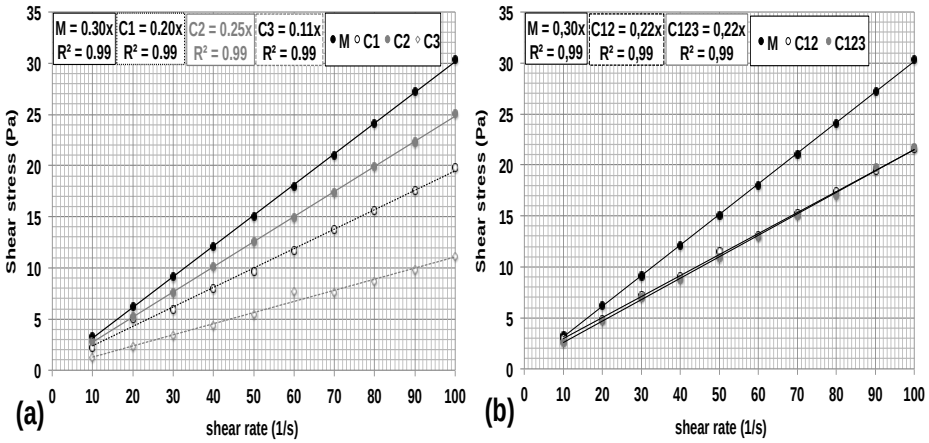

Figure 6. Rheograms of mixtures (a) M-C_1-C_2-C_3 (b) M-C_{12}-C_{123}.

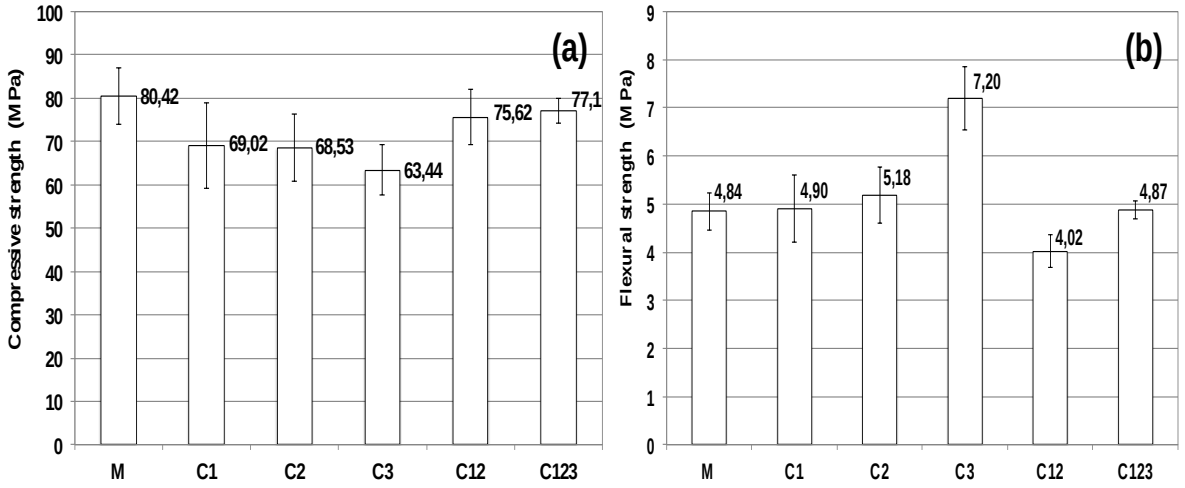

Figure 7. Mechanical properties of matrix and composites (a) compressive strength (b) flexural strength.

Figure 7b shows that the composites C_1 and C_2 have flexural strength similar to that of the reference matrix. However, composite C_3, containing the 0.05 *wt.*% of CNT_3, reaches a flexural strength 48% greater than the reference matrix and the composites C_1 and C_2. Navid et al. (2016) showed a considerable gain in flexural strength, ranging from 6 to 43%, while Xu, Liu, and Li (2015) published gains from 7.5 to 40%. The combination of CNT_1 and CNT_2 leads to a lower flexural strength, while the ternary mixture of CNT_1, CNT_2 and CNT_3 has a value similar to that of the reference matrix. The carbon nanotubes 1 and 2 (CNT_1) and (CNT_2) presented the highest volume of micrometric particles, probably in an agglomerated condition, as seen in the Figure 5a and b and their micrographies. These large particles cannot contribute to the improvement of the flexural strength, since under tensile strength they shall act as a defect on the microstructure of these composites. While the carbon nanotubes 3 (CNT_3) present the smallest volume of particles in the micrometric range (> 1 micra). In this way, the lower volume of these agglomerates, which shall act as a defect under tensile, reduce the negative effect of them on the flexural strength. When the content of carbon nanotubes 1 and 2 were combined in the composite C_{12}, the amount of these coarse agglomerates also increases. Similarly, the composite C_{123} presents a higher volume of these agglomerates from carbon nanotubes 1 and 2, which were majoritarian due to their higher percentage on the mixture. Other studies have also shown compressive or flexural strengths results lower than reference mixtures, without carbon nanotubes (Kumar, Kolay, Malla, & Mishra, 2012; Nasibulina et al., 2012; Manzur, Yazdani, & Emon, 2014; Szelag, 2017). Or even different mechanical behavior from composites under compression or flexural stress as published by Sbia, Peyvandi, Soroushian, and Balachandra (2014), and Hu et al. (2014).

Figure 8 and 13 show the scanning electron micrographies of the reference matrix and composites. Figure 8 shows the reference matrix, without carbon nanotubes, which have a dense structure. There is a spherical particle, probably a silica fume, covered by hydration products. Figure 9 shows composite C_1, a long fiber with a length greater than 10 μm was observed. The carbon nanotube is neither agglomerated, nor included in the cement matrix. The fiber is covering or adhering to the surface of the other particle. No evidence of pullout or breaking was identifiable. Figure 10 shows the composite C_2, which reveals the presence of hydration products on the fiber surface. The carbon nanotube 2 is clearly adhered to the surface of the matrix, and has a micrometric length greater than 10 μm. No pullout or the rupture of fibrous materials was observed. Figure 11 shows the composite C_3, the CNT_3 has a micrometric length, and the smallest diameter, when compared to CNT_1 and CNT_2. The particle has no rupture or pullout characteristics, being adhered to the matrix surface. It was also observed the presence of hydration products under the carbon nanotube. Figure 12 provides the micrography of the composite C_{12}, the identified carbon nanotube also has a micrometric length, and the growth of hydration products under its surface. The particle is also adhered to the cementitious matrix, without rupture or pullout characteristics. Figure 13 shows the composite C_{123}, the nano-silica is adhered to the surfaces of matrix. In this figure, it was observed a carbon nanotube included in the hydration products and adhered to the matrix surface. Hydration products, probably nano-silica particles covered by C-S-H or CH, were clearly observed.

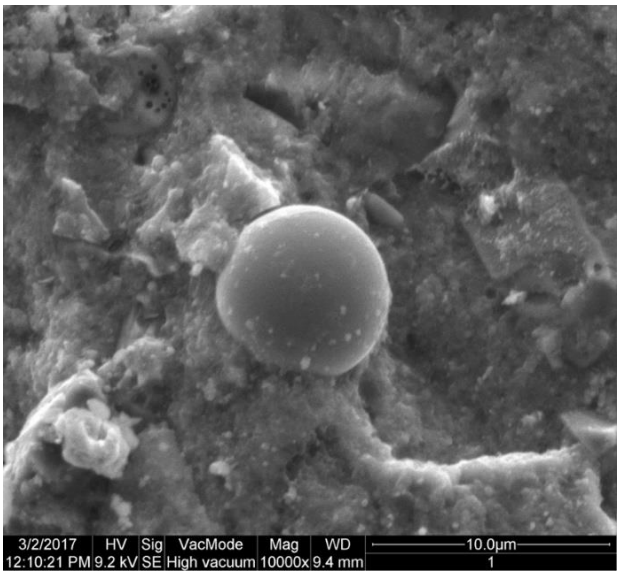

Figure 8. Scanning electron micrographies Reference Matrix.

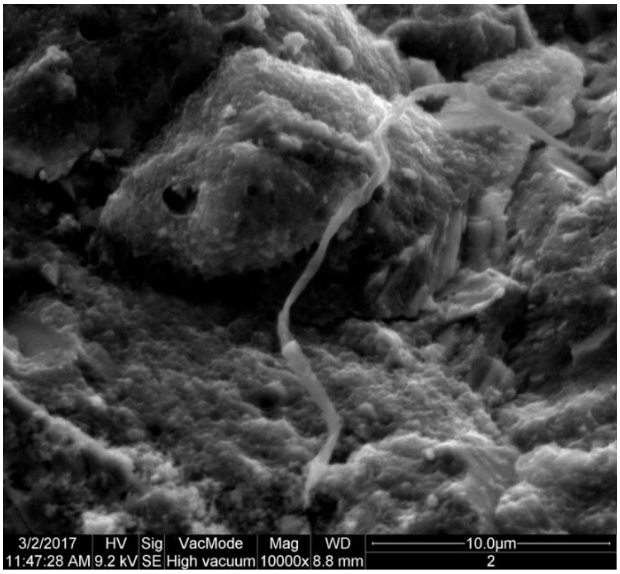

Figure 9. Scanning electron micrographies Composite C_1.

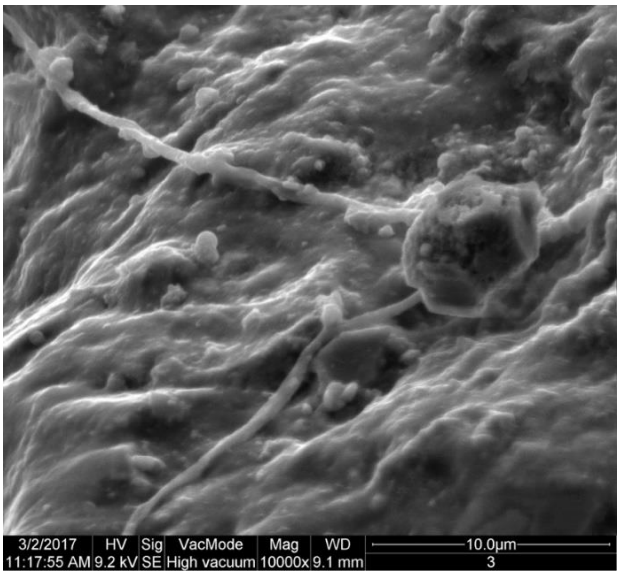

Figure 10. Scanning electron micrographies Composite C_2.

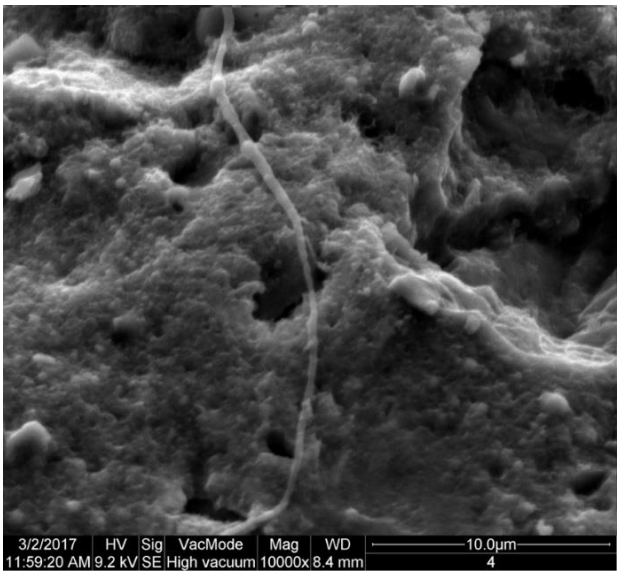

Figure 11. Scanning electron micrographies Composite C_3.

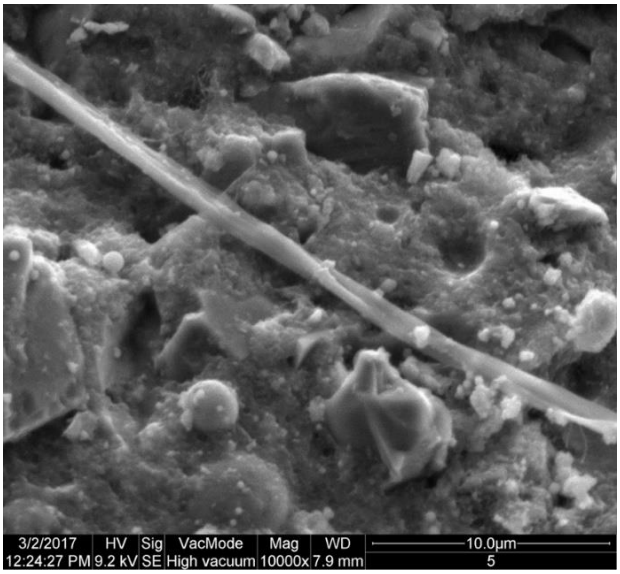

Figure 12. Scanning electron micrographies Composite C_{12}.

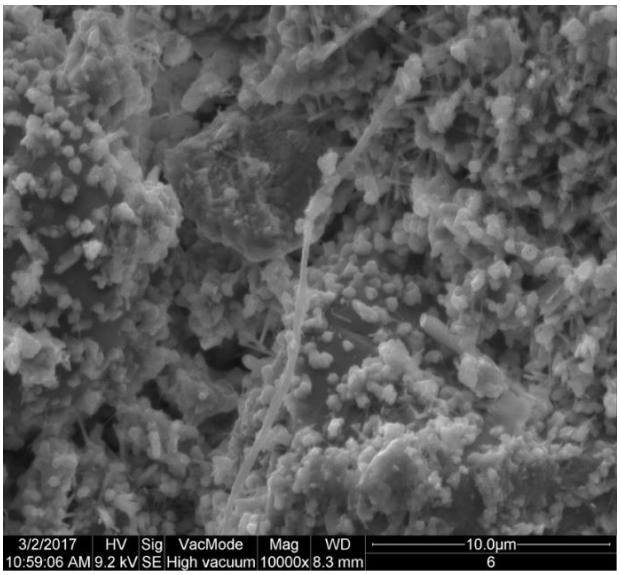

Figure 13. Scanning electron micrographies Composite C_{123}.

Conclusion

The particle size distributions measured by laser granulometry and electro-acoustic spectroscopy are comparable, and when used in conjunction with the specific surface area and electron transmission microscopy, helps to identify the finer or coarser carbon nanotube suspensions.

The viscosity of cement pastes decreases for the three different sizes of carbon nanotubes, as well as their binary and ternary mixtures. The compressive strength is reduced for the three different sizes of carbon nanotubes, as well as for their binary and ternary mixtures. The finer carbon nanotube improved the flexural strength of cement pastes.

The microstructural analysis of cement-based composites showed carbon nanotubes and nano-silica adhered under the surface of cement particles. It was also observed the nucleation of hydration products under the surfaces of carbon nanotubes and nano-silica.

Acknowledgements

The authors would like to thank the *Fundação Araucaria*, *Coordenação de Aperfeiçoamento de Pessoal de Nível Superior* (Capes) and *Conselho Nacional de Desenvolvimento Científico e Tecnológico* (CNPq).

References

Al-Rub, R. K. A., Ashour, A. I., & Tyson, B. M. (2012). On the aspect ratio effect of multi-walled carbon nanotube reinforcements on the mechanical properties of cementitious nanocomposites. *Construction and Building Materials, 35*, 647-655. DOI: https://doi.org/10.1016/j.conbuildmat.2012.04.086

American Society for Testing and Materials [ASTM]. (2018). *ASTM C674-13: Standard test methods for flexural properties of ceramic whiteware materials*. Montgomery, PA: ASTM.

Associação Brasileira de Normas Técnicas. (2017). *NBR 16605: Cimento Portland e outros materiais em pó - Determinação da massa específica*. Rio de Janeiro, RJ: ABNT.

Chang, C.-C., Hsu, I.-K., Aykol, M., Hung, W.-H., Chen, C.-C., & Cronin, S. B. (2010). A new lower limit for the ultimate breaking strain of carbon nanotubes. *ASC Nano, 4*(9), 5095-5010. DOI: https://doi.org/10.1021/nn100946q

Collins, F., Lambert, J., & Duan, W. H. (2012). The influences of admixtures on the dispersion, workability, and strength of carbon nanotube–OPC paste mixtures. *Cement and Concrete Composites, 34*(2), 201-207. DOI: https://doi.org/10.1016/j.cemconcomp.2011.09.013

Cwirzen, A., Habermehl-Cwirzen, H., & Pentalla, V. (2015). Surface decoration of carbon nanotubes and mechanical properties of cement/carbon nanotube composites. *Advances in Cement Research, 20*(2), 65-73. DOI: https://doi.org/10.1680/adcr.2008.20.2.65

El-Gamal, S. M. A., Hashem, F. S., & Amin, M. S. (2017). Influence of carbon nanotubes, nanosilica and nanometakaolin on some morphological-mechanical properties of oil well cement pastes subjected to elevated water curing temperature and regular room air curing temperature. *Construction and Building Materials, 146*, 531-546. DOI: https://doi.org/10.1016/j.conbuildmat.2017.04.124

Farooq, F., Akbar, A., Khushnood, R. A., Muhammad, W. L. B., Rehman, S. K. U., & Javed, M. F. (2020). Experimental investigation of hybrid carbon nanotubes and graphite nanoplatelets on rheology, shrinkage, mechanical, and microstructure of SCCM. *Materials, 13*(1), 230. DOI: https://doi.org/10.3390/ma13010230

Graybeal, B. (2014). Compression testing of ultra-high-performance concrete. *American Society for Testing and Materials, 4*(2), 102-112. DOI: https://doi.org/10.1520/ACEM20140027

Hawreen, A., Bogas, J. A., & Dias, A. P. S. (2018). On the mechanical and shrinkage behavior of cement mortars reinforced with carbon nanotubes. *Construction and Building Materials, 168*, 459-470. DOI: https://doi.org/10.1016/j.conbuildmat.2018.02.146

Hu, Y., Luo, D., Li, P., Li, Q., & Sun, G. (2014). Fracture toughness enhancement of cement paste with multi-walled carbon nanotubes. *Construction and Building Materials, 70*, 332-338. DOI: https://doi.org/10.1016/j.conbuildmat.2014.07.077

Jung, S.-H., Oh, S., Kim, S.-W., & Moon, J.-H. (2019). Effects of CNT dosages in cement composites on the mechanical properties and hydration reaction with low water-to-binder ratio. *Applied Sciences, 9*(21), 4630. DOI: https://doi.org/10.3390/app9214630

Kumar, S., Kolay, P., Malla, S., & Mishra, S. (2012). Effect of multiwalled carbon nanotubes on mechanical strength of cement paste. *Journal of Materials in Civil Engineering, 24*(1), 84-91. DOI: https://doi.org/10.1061/(ASCE)MT.1943-5533.0000350

Konsta-Gdoutos, M.S., Metaxa, Z.S., Shah, S.P. (2010a). Multi-scale mechanical and fracture characteristics and early-age strain capacity of high-performance carbon nanotube/cement nanocomposites. *Cement and Concrete Composites*, *32*, 110-115. DOI: https://doi.org/10.1016/j.cemconcomp.2009.10.007

Konsta-Gdoutos, M.S., Metaxa, Z.S., Shah, S.P. (2010b). Highly dispersed carbon nanotube reinforced cement-based materials. *Cement and Concrete Research*, *40*, 1052-1059. DOI: https://doi.org/10.1016/j.cemconres.2010.02.015

Leonavičius, D., Pundienė, I., Giedrius, G., Pranckevičienė, J., Kligys, M., & Kairytė, A. (2018). The effect of multi-walled carbon nanotubes on the rheological properties and hydration process of cement pastes. *Construction and Building Materials, 189*, 947-954. DOI: https://doi.org/10.1016/j.conbuildmat.2018.09.082

Manzur, T., Yazdani, N., & Emon, A. B. (2014). Effect of carbon nanotube size on compressive strengths of nanotube reinforced cementitious composites. *Journal of Materials, 2014*, 960984. DOI: https://doi.org/10.1155/2014/960984

Medeiros, M. H. F., Dranka, F., Mattana, A. J., & Costa, M. R. M. M. (2015). Portland cement composites with carbon nanotubes (CNT) addition: Properties in freshly state and compressive strength. *Matéria, 20*(1), 127-144. DOI: https://doi.org/10.1590/S1517-707620150001.0014

Mendoza, O., Sierra, G., & Tóbon, J. I. (2014). Effect of the reagglomeration process of multi-walled carbon nanotubes dispersions on the early activity of nanosilica in cement composites. *Construction and Building Materials, 54*, 550-557. DOI: https://doi.org/10.1016/j.conbuildmat.2013.12.084

Meng, W., & Khayat, K. H. (2016). Mechanical properties of ultra-high-performance concrete enhanced with graphite nanoplatelets and carbon nanofibers. *Composites Part B: Engineering, 107*, 113-122. DOI: https://doi.org/10.1016/j.compositesb.2016.09.069

Nanostructured & Amorphous Materials. (2021). Retrieved from https://nanoamor.com

Nasibulina, L. I., Anoshkin, I. V., Nasibulin, A. G., Cwirzen, A., Penttala, V., & Kauppinen, E. I. (2012). Effect of carbon nanotube aqueous dispersion quality on mechanical properties of cement composite. *Journal of Nanomaterials, 2012*, 169262. DOI: https://doi.org/10.1155/2012/169262

Navid, R., Vasilyev, G., Shtein, M., Peled, A., Zussman, E., & Regev, O. (2016). The multiple roles of a dispersant in nanocomposite systems. *Composites Science and Technology, 133*, 192-199. DOI: https://doi.org/10.1016/j.compscitech.2016.07.008

Sbia, L. A., Peyvandi, A., Soroushian, P., & Balachandra, A. M. (2014). Optimization of ultra-high-performance concrete with nano- and micro-scale reinforcement. *Cogent Engineering, 1*(1), 990673. DOI: https://doi.org/10.1080/23311916.2014.990673

Sikora, P., Elrahman, M. A., Chung, S.-Y., Cendrowski, K., Mijowska, E., & Stephan, D. (2019). Mechanical and microstructural properties of cement pastes containing carbon nanotubes and carbon nanotube-silica core-shell structures, exposed to elevated temperature. *Cement and Concrete Composites, 95*, 193-204. DOI: https://doi.org/10.1016/j.cemconcomp.2018.11.006

Skripkiunas, G., Karpova, E., Barauskas, I., Bendoraitiene, J., & Yakovlev, G. (2018). Rheological properties of cement pastes with multiwalled carbon nanotubes. *Advances in Materials Science and Engineering,* 2018, 8963542. DOI: https://doi.org/10.1155/2018/8963542

Sobolkina, A., Mechtcherine, V., Khavrus, V., Maier, D., Mende, M., Ritschel, M., & Leonhardt, A. (2012). Dispersion of carbon nanotubes and its influence on the mechanical properties of the cement matrix. *Cement and Concrete Composites, 34*(10), 1104-1113. DOI: https://doi.org/10.1016/j.cemconcomp.2012.07.008

Szelag, M. (2017). Mechano-physical properties and microstructure of carbon nanotube reinforced cement paste after thermal load. *Nanomaterials, 7*(9), 267. DOI: https://doi.org/10.3390/nano7090267

Xu, S., Liu, J., & Li, Q. (2015). Mechanical properties and microstructure of multi-walled carbon nanotube-reinforced cement paste. *Construction and Building Materials, 76*, 16-23. DOI: https://doi.org/10.1016/j.conbuildmat.2014.11.049

Yakovlev, G. I., Skripkiunas, G., Polianskich, I. S., Lahayne, O., Eberhardsteiner, J., Urkhanova, L. A., ... Sen'kov, S. A. (2017). Modification of cement matrix using carbon nanotube dispersions and nanosilica. *Procedia Engineering, 172*, 1261-1269. DOI: https://doi.org/10.1016/j.proeng.2017.02.148

Yazdanbakhsh, A., & Grasley, Z. (2012). The theoretical maximum achievable dispersion of nanoinclusions in cement paste. *Cement and Concrete Research, 42*(6), 798-804. DOI: https://doi.org/10.1016/j.cemconres.2012.03.001